Inelasticity distribution of hadron-Pb collisions in the energy region exceeding 10^{14} eV from mountain cosmic ray experiments

C. R. A. Augusto,[1] S. L. C. Barroso,[2] Y. Fujimoto,[3] V. Kopenkin,[1,4] M. Moriya,[3] C. E. Navia,[1] A. Ohsawa,[5] E. H. Shibuya,[2] and M. Tamada[6]

[1]*Instituto de Física, Universidade Federal Fluminense, 24020-130 Niteroi, Rio de Janeiro, Brazil*
[2]*Instituto de Física Gleb Wataghin, UNICAMP, 13083-970 Campinas, São Paulo, Brazil*
[3]*Advanced Research Center for Science and Engineering, Waseda University, Tokyo, 169 Japan*
[4]*Institute of Nuclear Physics, Moscow State University, 119899, Moscow, Russia*
[5]*Institute for Cosmic Ray Research, University of Tokyo, Tanashi, Tokyo, 188 Japan*
[6]*Faculty of Science and Technology, Kinki University, Higashi-Osaka, Osaka, 577 Japan*

(Received 31 December 1998; published 8 December 1999)

The inelasticity distribution of hadron-lead collisions in the energy region exceeding 10^{14} eV is estimated on the basis of 66 events, induced by cosmic ray hadrons and detected at high mountain altitudes at Pamir (4300 m, 595 g/cm^2). The distribution of the best fitting is approximated as $g(K)dK=[\alpha(1-K)^{m_1-1}+\beta K^{m_2-1}]dK$, where $m_1=0.5$, $m_2=1.125$, $\alpha=0.26$, $\beta=0.55$, giving $\langle K\rangle=0.60$. The errors of the parameters are discussed in the text. The distribution is compared with those which are based on theoretical models.

PACS number(s): 96.40.De, 13.85.Tp

I. INTRODUCTION

The concept of the inelasticity is used widely in discussing the features of multiple particle production [1]. It is one of the important issues from the following points of view.

The inelasticity distribution, the energy dependence of the average inelasticity, etc., imposes limitations on the theoretical models of multiple particle production. For example, the energy dependence of the average inelasticity, predicted by theoretical models, varies from strongly decreasing to strongly increasing [2–7].

Study of cosmic ray events in the energy region exceeding 10^{15} eV is particularly important both for particle physics and for astrophysics, because this region exceeds the energies of existing accelerators and the energy spectrum of primary cosmic rays has a bend. This study can be made by analyzing high energy cosmic ray phenomena in the atmosphere, and the inelasticity is indispensable in the analysis because it is one of the essential factors which govern cosmic ray propagation in the atmosphere.

The inelasticity is defined as

$$K=\frac{\sum E_i}{E_0},$$

where E_0 is the energy of the incident particle and E_i's are the energies of the produced particles in multiple particle production, assuming that the particles in the final state consist of one surviving particle and a number of produced particles.

It is observed in p-p collisions at low energies (e.g., $E_0<200$ GeV) that the final state of multiple particle production consists of a surviving nucleon and a number of produced particles, mainly pions. This view of surviving and produced particles is applicable to $\pi^{\pm}-p$ collisions, too, under the restrictions that (1) the energy spectrum of produced particles, expressed by the parameter $x\equiv E/E_0$, is identical in p-p and in π-p collisions, and (2) the surviving particle can be one of π^+, π^- and π^0 through the charge exchange process. As a first approximation we can assume that this simple view is valid in the high energy region where baryons exist among the produced particles,[1] at least from the energy flow point of view.

The inelasticity was introduced first from the fact that the attenuation of cosmic rays is not as strong as expected by the extremely violent nuclear interactions (i.e., $K=1.0$), and was estimated to be 0.5 approximately. Later the energies of the produced charged particles in multiple particle production were measured by bubble chamber experiments, which showed that the inelasticity has an almost uniform distribution between 0 and 1,[2] leading to $\langle K\rangle=0.5$ [9]. Van Hove and Pokorski described the data by the picture of independent cluster production which can be related to a quark-gluon picture of nucleon structure [10].

Feynman speculated that the energy spectrum of produced particles in multiple particle production is not dependent on the primary energy as $\sqrt{s}\to\infty$, when it is expressed by the parameter[3]

$$x^*\equiv\frac{2p_{\parallel}^*}{\sqrt{s}}\simeq\frac{E}{E_0}\equiv x$$

[1]It is not always possible in this case to identify the surviving particle among the final state particles experimentally. Therefore, some are interested in ''the most energetic particle'' or ''a leading particle'' instead of the surviving particle, aiming at a well-defined concept [8]. However, then we would lose a simple description of the phenomenon instead.

[2]There is a peak at $K\sim 0$ due to the diffraction process.

[3]It had been pointed out by the emulsion chamber experiments that the energy spectrum of produced particles is described by E/E_0, which was called the similarity relation [11].

under the assumptions of constant cross section and constant transverse momenta of produced particles [12]. If this is true, it follows that the average inelasticity remains 0.5 at high energies. Due to the importance of this Feynman scaling law in governing the characteristics of high energy hadron interactions and due to the usefulness of extrapolating the data of accelerator experiments to a higher energy region, the validity of the law was examined by many experimental groups. They reached the conclusion that the law is valid up to $\sqrt{s}=63$ GeV, the maximum available energy at that time [13].

At still higher energies ($\sim 10^{14}$ eV), however, it is shown by examining the available accelerator data that the scaling law is violated [14]. That is, the energy spectrum of produced particles is enhanced in the central region and suppressed in the forward region. The violation of the law in the high energy region was pointed out first by emulsion chamber experiments [15–17]. The UA5 Collaboration made a simulation code of multiple particle production, which reproduces experimental results in the central rapidity region at the CERN Super Proton Synchrotron (SPS) $\bar{p}p$ collider at the energies $\sqrt{s}=53$, 200, 546, and 900 GeV. The UA5 code predicts a suppression of particle production in the forward region compared with the scaling law, resulting in $\langle K\rangle = 0.42$ at $\sqrt{s}=546$ GeV [18].[4]

In the energy region exceeding 10^{14} eV there is no data on the inelasticity of hadron-hadron collisions from direct observation, because available high energy accelerators are all of the collider-type, so the surviving hadron and/or the particles produced in the forward region are not easy to be observed. The data from hadron-nucleus collisions are available only at low energies.

Hence, in the present paper, we estimate the inelasticity in the energy region exceeding 10^{14} eV from the data of a cosmic ray experiment. The experimental data are from hadron-Pb collisions observed by thick emulsion chambers, exposed to cosmic rays at high mountain altitudes at Pamir. The basic idea is that a hadron, incident upon the chamber, makes collisions successively in the chamber, and that the showers produced in these collisions are detected individually. One can estimate the energies of the individual collisions, the total energy sum of them, and finally the energy of the incident hadron.

The advantages of the present work are the following: (1) the inelasticity distribution can be discussed in the energy region of ~ 200 TeV. (2) the target nucleus effect of the inelasticity in the hadron-nucleus collision can be discussed in the most amplified way by studying hadron-Pb collisions; and (3) the method of analysis makes it possible to discuss the inelasticity of hadron-nucleon collisions, too.

[4]The value is for all inelastic events. One should be careful of the difference between those of ''all inelastic'' and ''non-single-diffractive.'' Needless to say, the value is larger for non-single-diffractive events, i.e., ~ 0.5.

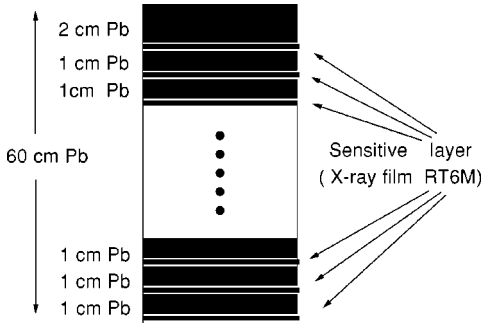

FIG. 1. Schematic structure of Pamir thick lead chamber. The thickness of the chamber is 60 cm Pb or 3.2 mean free path of inelastic collision of nucleon. The sensitive layers of Russian x-ray film RT-6M are inserted at every 1 cm of lead plate after 2 cm lead from the top.

II. OBSERVATION OF HADRONS BY EMULSION CHAMBER

A. Emulsion chamber

The emulsion chamber is a shower detector of sensitive layers of x-ray films and/or nuclear emulsion plates, interposed by lead plates (Fig. 1). (We will refer hereafter only to x-ray films which are the only sensitive material used in the present Pamir chambers.) The chamber detects cascade showers and allows one to determine their energies. A high energy particle of the electromagnetic component produces a bundle of electrons and photons, called a ''cascade shower,'' in the chamber through the chain of electromagnetic interactions. A cascade shower develops through several layers of lead plates (each of 1 cm thickness) before dying out due to the energy losses. Since x-ray film is sensitive to charged particles, electrons in the cascade shower are recorded. This bundle of electrons appears on x-ray film after photographic development as a small dark spot (~ 100 μm) . Reconstruction of all the spot positions in the chamber makes it possible to identify all the cascade showers recorded in x-ray films.

The energy of a cascade shower is determined through the photometric measurement of shower spots in x-ray films. The opacity of the shower spot D, called ''darkness,'' is measured by the microphotometer with the square aperture of 200 μm$\times$200 μm. The development of the darkness along the depth of the chamber, called the ''transition curve,'' is compared with those of the cascade theory [19], calculated for various incident energies.

A high energy hadron incident upon the chamber, causes multiple particle production in the chamber through nuclear collisions with Pb nuclei. The electromagnetic component among the produced particles (mainly due to the decays of π^0's) initiates a cascade shower. Therefore, the observed energy of the hadron-induced shower is not that of the incident hadron, E_h, but that of the produced electromagnetic component, i.e., $E^{(\gamma)}=k_\gamma E_h$ with $k_\gamma<1$.

The detection threshold energy of showers in the emulsion chamber is *several* TeV, depending on the quality of x-ray films, condition of exposure, condition of photographic development, etc. The general problems of the determination of energy from measured darkness D is described in the paper of Arisawa *et al.* [20].

TABLE I. Details of the Pamir thick lead chambers.

Chamber	PB-68	PB-69	PB-72	PB-73	Total
Area (m^2)	9	8	20	20	57
Years of exposure	88–89	88–89	89–91	89–91	
Thickness (cm Pb)	60	60	60	60	
No. of sensitive layers	58	58	59	59	
Hadrons in family	4 (0)	5 (1)	12 (3)	11 (1)	32 (5)
Hadrons of single arrival	5 (1)	6 (3)	11 (1)	12 (3)	34 (8)
Total	9 (1)	11 (4)	23 (4)	23 (4)	66 (13)

B. Pamir thick lead chambers

The Pamir thick lead chambers are constructed at Pamir (4300 m, at an atmospheric depth of 595 g/cm^2) by the Pamir Collaboration [20,21]. They have distinguished characteristics of large thickness (60 cm Pb or 3.2 mean free paths of inelastic collision length of nucleons) and uniform structure (see Fig. 1). The former assures an almost 100% collision probability of hadrons in the chamber, and consequently, γ rays[5] and hadrons, incident upon the chamber, are detected in a minimum-biased way. The latter permits a uniform detection of showers all over the depth of the chamber and the simplest way of energy determination. Table I shows details of the chambers where 66 events for the present analysis were observed.

The initial analysis of high energy events,[6] observed in the present chambers, has been made in Ref. [22]. This work is practically the first work based on reasonable statistics of families with minimum-biased hadron data,[7] because the cosmic ray data, available so far, have concerned mainly γ rays in the families, due to the very limited thickness of chambers.

C. Hadrons in the Pamir thick lead chambers — successive interactions

A hadron, incident upon the chamber, causes a nuclear collision — multiple particle production — in the chamber. The surviving hadron and the produced hadrons undergo nuclear collisions again at various depths in the chamber (see Fig. 2). The process is repeated in the chamber until the hadrons, incident and produced, leave the chamber. Electromagnetic showers, produced in these collisions in the chamber with energies exceeding the detection energy threshold E_{th} are recorded in the x-ray emulsion chamber.

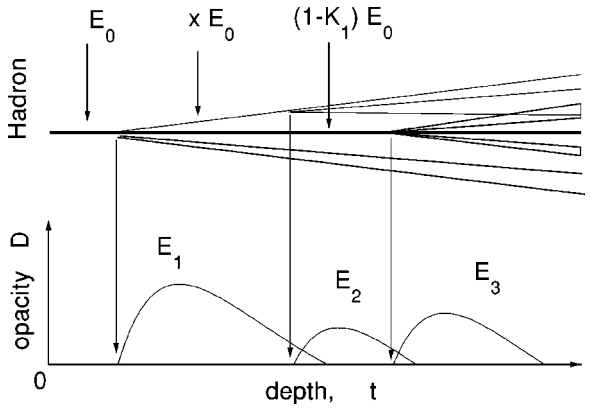

FIG. 2. Illustration of successive interactions in the chamber. The hadron (the bold solid line), incident upon the chamber, causes a nuclear interaction in the chamber (the first interaction) to produce the electron shower with energy E_1. The produced pions (the thin solid lines) cause a nuclear collision (the second interaction) to produce the shower with E_2. The surviving hadron (the bold solid line) causes a nuclear collision again (the third interaction) to produce the shower with E_3. Successive interactions of three showers are illustrated in the chamber.

Consequently, a single high energy hadron, incident upon the chamber, produces in the chamber n showers ($n=1,2,\ldots$) which have the appearance of aligning longitudinally and having the same direction. An event with $n \geqslant 2$ is called a ''successive interaction event,'' and one with $n=1$ is called a ''single shower.''

D. Distribution of z

Let us denote the energy of the first, the second, . . . , shower in the event by $E_1, E_2, \ldots$, and that of the incident hadron by E_0 (Fig. 2). The parameter z is defined as

$$z \equiv \frac{E_1}{\sum E_i}$$

which is a measure of the inelasticity of the interaction of the first shower.

The distribution of z is shown in Fig. 3. It is based on 66 experimental events with $\Sigma E_i > 30$ TeV and an energy detection threshold $E_{th}=4$ TeV. Among these 66 events, 13 are single-shower events, and the remaining 53 events are those with successive interactions.[8] A set of 66 events consists of

[5]The electromagnetic component (electron and photon) are collectively called ''γ rays'' in emulsion chamber experiments.

[6]The minimum-biased events database of unaccompanied incident showers and families has been created during the stay of V. Kopenkin at Waseda University.

[7]A ''family'' is a bundle of showers of parallel incidence, observed in the emulsion chamber. Those showers are originated by the particles which are produced by nuclear interaction(s) in the atmosphere above the chamber.

[8]In our previous report [23], we made an analysis of 74 events of successive interactions. We found, however, that classification between single-shower events and two-showers event cannot be made easily because, in most of the cases, the second shower has an energy near the detection threshold. We make a reanalysis in the present report including single-shower events. The decrease of the number of events of successive interactions from 74 to 53 is due to the revised energy calibration of x-ray films.

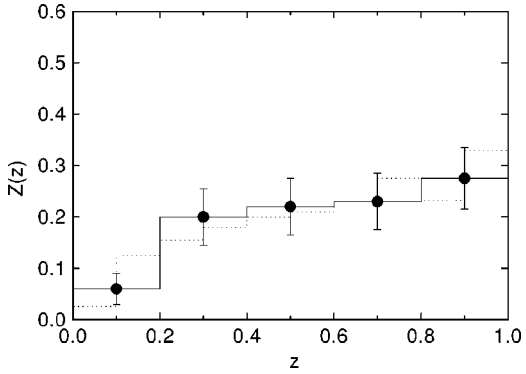

FIG. 3. Histogram of z, where z is the ratio of the energy of the first shower to the energy sum of all the showers (see the text). The solid line is experiment (errors are only due to the number of events) and the dashed line is the best fitting, based on the assumed inelasticity distribution.

32 hadrons in families and 34 of single arrival (they consist of successive interaction events as well as single-shower events). Due to the limited statistics of events, the histogram has large bins.

III. DISTRIBUTION OF INELASTICITY

In this section we define the inelasticity in relation to the energy spectrum of produced particles in hadron-Pb collisions, show the relation between the z distribution and the inelasticity distribution, and compare the experimental and calculated z distributions to discuss the inelasticity distribution.

(i) Energy spectrum of produced particles in hadron-Pb collisions. The final state of hadron-Pb collision consists of the surviving hadron and the produced particles. For the sake of simplicity we assume that all the produced particles are pions, which have three charge states with equal probability (i.e., $c=1/3$). According to the experimental data, the energy spectrum of produced particles from a hadron-nucleus collision is similar to that from a p-p collision in the forward region and is enhanced in the central region due to the target nucleus effect. The energy spectrum of produced *charged* pions is expressed as

$$\begin{aligned}\varphi(E_0,E,\xi_1,\xi_2)dE &= (1-c)(a+1)\xi_1\frac{(1-x)^a}{x}dx+(1-c)(1-\xi_1)\xi_2 \times\frac{\delta(x-\epsilon)}{\epsilon}dx \\ &\equiv \varphi(x,\xi_1,\xi_2)dx, \end{aligned} \tag{1}$$

where $x=E/E_0$.

The first term is the energy spectrum of the produced particles in the forward region. We assume it to be the same as an empirical formula of the energy spectrum of produced particles in p-p collision. In the formula the parameter $a=4.0$ is empirical, $1-c=2/3$ signifies the fraction of charged pions, $(a+1)$ is the normalization, and ξ_1 is the partial inelasticity (corresponding to the produced particles in the forward region), details of which are described below.

The second term corresponds to the enhancement of the produced particles in the central region in hadron-Pb collision. The delta function $\delta(x-\epsilon)$ signifies that the produced particles in the central region are assumed to have monochromatic energies of $x=\epsilon(\ll 1)$. Consequently, the second term makes the total inelasticity larger than ξ_1.

The term $(1-\xi_1)\xi_2$ signifies that a fraction ξ_2 $(0\leqslant\xi_2\leqslant 1)$ of the rest of the energy, $1-\xi_1$, is used to produce the particles in the central region. These particles do not participate in the nuclear cascade process in the chamber, because of their low energies, but serve to increase the inelasticity. ξ_1 and ξ_2 have distributions of $f_1(\xi_1)d\xi_1$ and $f_2(\xi_2)d\xi_2$ between ξ of 0 and 1, and are normalized to 1.

Integration of $\varphi(x,\xi_1,\xi_2)xdx$ is the (normalized) radiated energy of the charged produced particles in the collision, which is related to the (charged) inelasticity, $(1-c)K$. That is,

$$\int_0^1 \varphi(x,\xi_1,\xi_2)xdx=(1-c)[\xi_1+\xi_2(1-\xi_1)]=(1-c)K.$$

Hence we have

$$K=\xi_1+(1-\xi_1)\xi_2.$$

Consequently the inelasticity distribution is given by

$$g(K)dK=dK\int \delta[K-\xi_1-(1-\xi_1)\xi_2] \times f_1(\xi_1)d\xi_1 f_2(\xi_2)d\xi_2. \tag{2}$$

We assume the following for $f_1(\xi)$ and $f_2(\xi)$:

$$f_1(\xi)=N[\alpha(1-\xi)^{m_1-1}+\beta\xi^{m_2-1}], \quad \left(\frac{1}{N}=\frac{\alpha}{m_1}+\frac{\beta}{m_2}\right) \tag{3}$$

and:

$$f_2(\xi)=\frac{1}{2\delta}\theta(2\delta-\xi), \tag{4}$$

where $\theta(x)$ is the step function and $\alpha,\beta,m_1,m_2>0$, and $\delta<0.5$.

The distribution $f_1(\xi)d\xi$ with adjustable parameters α,β,m_1,m_2 signifies that the partial inelasticity of the produced particles in the forward region, ξ_1, is assumed to be of hammock shape between 0 and 1. The distribution $f_2(\xi)d\xi$ assumes that the fraction ξ_2 is distributed uniformly between 0 and 2δ where δ is an adjustable parameter. Then we have

$$g(K)dK=dK\frac{N}{2\delta}\int_0^{\min(K,2\delta)}\left[\alpha\left(\frac{1-K}{1-\xi}\right)^{m_1-1}+\beta\left(\frac{K-\xi}{1-\xi}\right)^{m_2-1}\right]\frac{d\xi}{1-\xi}. \tag{2'}$$

All the parameters of $\alpha,\beta,m_1,m_2,\delta$ are not independent, but the two prefixed conditions, the normalization of the distribution and the mean value of the inelasticity, are not sufficient to determine all the values of the parameters. In other words, even after specifying the average inelasticity, there are a variety of inelasticity distributions.

The distributions have average values expressed as

$$\langle \xi_1 \rangle = N\left[\frac{\alpha}{m_1+1}+\frac{\beta}{m_2+1}\right] \text{ and } \langle \xi_2 \rangle = \delta,$$

$$\langle K \rangle = \int_0^1 K\delta[K-\xi_1-(1-\xi_1)\xi_2]f_1(\xi_1)d\xi_1 f_2(\xi_2)d\xi_2$$
$$= \langle \xi_1 \rangle + (1-\langle \xi_1 \rangle)\langle \xi_2 \rangle \equiv K_1 + K_2.$$

(ii) Z distribution. The nucleon of energy E_0, incident upon the chamber, makes a first interaction with inelasticity $K(\xi_1,\xi_2)$. After the collision the surviving nucleon has energy

$$(1-K)E_0 \text{ with } K=\xi_1+(1-\xi_1)\xi_2,$$

and the charged pions, produced by the collision, have an energy spectrum

$$\varphi(x,\xi_1,\xi_2)dx.$$

The surviving nucleon and the charged pions, produced in the collision, undergo the nuclear cascade process. The total observed energy of the showers, produced by the process, is denoted as $R(E_0,K)$. It is calculated in an analytic way by solving the diffusion equation of the process (Appendix), because a considerable number of particles are involved in the process which reduces the fluctuations reasonably.

As we have

$$E_1 = cKE_0 \text{ and } \sum E_i = E_1 + R(E_0,K),$$

the z distribution is given as

$$Z(z)dz = \int \delta\left(z-\frac{cKE_0}{\sum E_i}\right) f_1(\xi_1)d\xi_1 f_2(\xi_2)d\xi_2$$
$$\times \theta(cKE_0-E_{th})\theta\left(\sum E_i - E_{\rm tot}(th)\right)$$

with $K=\xi_1+(1-\xi_1)\xi_2$. The two θ functions express the experimental conditions (1) the first shower is detected and (2) the total observed energy exceeds $E_{\rm tot}(th)=30$ TeV.

When the incident energy of hadron is distributed as

$$\gamma N\left(\frac{E_0}{E_{\rm tot}(th)}\right)^{-\gamma-1} d\left(\frac{E_0}{E_{\rm tot}(th)}\right),$$

then we have

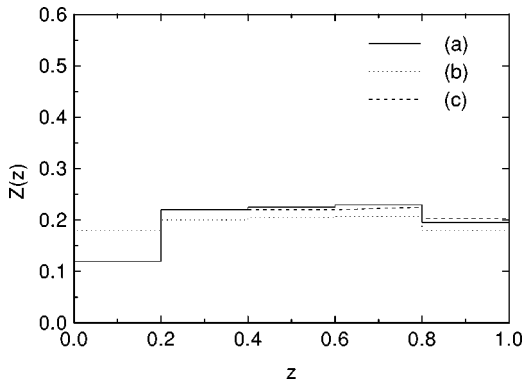

FIG. 4. Histogram of the z distribution, based on the assumed inelasticity distribution. The line (a) is the case of $m_1=2.0$, $m_2=2.0$, $\alpha=1.0$, $\beta=1.0$ and $\delta=0.0$, which gives $\langle K \rangle = 0.5$. The lines (b) and (c) are the cases where the experimental conditions of E_{th} and $E_{\rm tot}(th)$ are ignored, for the parameters of the line (a), respectively.

$$Z(z)dz = \int_0^c \int \delta\left(z-\frac{cK}{cK+R(E_0,K)/E_0}\right)$$
$$\times f_1(\xi_1)d\xi_1 f_2(\xi_2)d\xi_2 \gamma N u^{\gamma-1}du$$
$$\times \theta\left(cK-\frac{E_{th}}{E_0}\right)\theta\left(cK+\frac{R(E_0,K)}{E_0}-u\right), \quad (5)$$

with $u=E_{\rm tot}(th)/E_0$.

Figure 4 presents the analytical calculation of the z distribution for

$$m_1=2.0,\ m_2=2.0,\ \alpha=1.0,\ \beta=1.0, \text{ and } \delta=0.0$$

in Eqs. (3) and (4). The effects of E_{th} and $E_{\rm tot}(th)$ are also examined in Fig. 4 by removing their corresponding θ functions, drawn as lines (b) and (c), respectively. The threshold energy of the shower detection has an effect in the region of small z, while the total observed energy affects it slightly.

(iii) Comparison of experimental data with calculation. The dispersion between the experimental data and the calculated curve is defined as

$$D=\sum_{i=1}^{5}[y_i(\exp)-y_i(\text{cal})]^2,$$

where y_i is the value of the distribution at $z=z_i$. Table II shows D for the possible combination of the parameters m_1, m_2, α, β, and δ.

Figure 5 shows the contour of D on the plane of

$$K_1=\langle \xi_1 \rangle \text{ and } K_2=\langle (1-\xi_1)\xi_2 \rangle \ (\langle K \rangle = K_1+K_2)$$

in the ξ of $m_1=1.5$. We define the region with $D<0.01$ as good fitting, and call it the ''allowed'' region. One can see at once that $\langle K_1 \rangle = 0.6^{+0.02}_{-0.05}$ is in the allowed region, and $K_2 < 0.07$ is allowed, keeping $\langle K \rangle = 0.6$.

To discuss the shape of the inelasticity distribution, we took the case of $\langle K \rangle = 0.6$ (with $K_1=0.6$ and $K_2=0$, which is located aprroximately at the center of the contour. Figure 6

TABLE II. Dispersion of the z distributions D.

K_1	K_2	m_1	m_2	α	β	δ	D
0.4	0.0	0.500	0.222	0.225	0.122	0.000	1.02×10^{-2}
0.4	0.0	1.500	0.667	0.731	0.342	0.000	4.82×10^{-2}
0.4	0.0	2.500	1.111	1.313	0.528	0.000	5.52×10^{-2}
0.4	0.1	0.500	0.222	0.225	0.122	0.167	2.67×10^{-2}
0.4	0.1	1.500	0.667	0.731	0.342	0.167	3.20×10^{-2}
0.4	0.1	2.500	1.111	1.313	0.528	0.167	3.74×10^{-2}
0.4	0.2	0.500	0.222	0.225	0.122	0.333	4.23×10^{-3}
0.4	0.2	1.500	0.667	0.731	0.342	0.333	2.29×10^{-2}
0.4	0.2	2.500	1.111	1.313	0.528	0.333	2.51×10^{-2}
0.4	0.3	0.500	0.222	0.225	0.122	0.500	2.47×10^{-2}
0.4	0.3	1.500	0.667	0.731	0.342	0.500	2.52×10^{-2}
0.4	0.3	2.500	1.111	1.313	0.528	0.500	2.43×10^{-2}
0.5	0.0	0.500	0.500	0.250	0.250	0.000	6.69×10^{-3}
0.5	0.0	1.500	1.500	0.750	0.750	0.000	1.55×10^{-2}
0.5	0.0	2.500	2.500	1.250	1.250	0.000	9.93×10^{-3}
0.5	0.1	0.500	0.500	0.250	0.250	0.200	1.42×10^{-3}
0.5	0.1	1.500	1.500	0.750	0.750	0.200	1.17×10^{-2}
0.5	0.1	2.500	2.500	1.250	1.250	0.200	4.10×10^{-3}
0.5	0.2	0.500	0.500	0.250	0.250	0.400	2.34×10^{-2}
0.5	0.2	1.500	1.500	0.750	0.750	0.400	3.46×10^{-2}
0.5	0.2	2.500	2.500	1.250	1.250	0.400	3.02×10^{-2}
0.6	0.0	0.500	1.125	0.257	0.546	0.000	1.83×10^{-3}
0.6	0.0	1.500	3.375	0.692	1.817	0.000	4.97×10^{-3}
0.6	0.0	2.500	5.625	1.105	3.138	0.000	2.30×10^{-2}
0.6	0.1	0.500	1.125	0.257	0.546	0.250	2.05×10^{-2}
0.6	0.1	1.500	3.375	0.692	1.817	0.250	2.90×10^{-2}
0.6	0.1	2.500	5.625	1.105	3.138	0.250	2.72×10^{-2}
0.7	0.0	0.500	2.722	0.242	1.403	0.000	3.02×10^{-2}
0.7	0.0	1.500	8.167	0.583	4.991	0.000	7.02×10^{-2}
0.7	0.0	2.500	13.611	0.896	8.731	0.000	1.02×10^{-1}

shows that D has minimum at $m_1=0.5$ in this case. Therefore, the inelasticity distribution of the best fit is attained by the set of parameters

$$m_1=0.5, m_2=1.125, \alpha=0.26, \beta=0.55, \text{ and } \delta=0.0,$$

where $\langle K\rangle=0.6$ (with $K_1=0.6$ and $K_2=0.0$).

According to statistics, the quantity

$$\chi^2\equiv\sum_{i=1}^{5}\left(1-\frac{y_i(\text{cal})}{y_i(\text{expt})}\right)^2\Bigg/\frac{(\Delta y_i}{y_i(\text{exp})}{}^2$$

$$\times[\Delta y_i:\ \text{dispersion of } y_i(\text{exp})]$$

follows the χ^2 distribution with degree of freedom $n_D=4$. Because $\chi^2=0.71$ ($n_D=4$) for the z distribution of the best fitting, the confidence level is $\sim100\%$. It is simply because the dispersion of the experimental data is large due to small statistics of the events.

The inelasticity distribution of the best fitting is shown in Fig. 7. One can see that the distributions of $m_1=1.0,1.5,2.0$ (with $K_1=0.6$ and $K_2=0$), and even that of $m_1=0.5$ (with $K_1=0.55$ and $K_2=0.05$, leading to $\langle K\rangle=0.6$), are similar in shape. All of these cases belong to the allowed region.

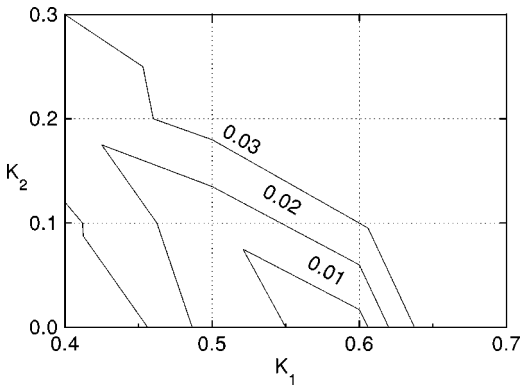

FIG. 5. Contour of the dispersion D between the z distributions of the experiment and the calculation for the various values of K_1 and K_2 ($m_1=1.5$). Defining the region $D<0.01$ as ''allowed'' (meaning ''good fitting''), one comes to the conclusion that $\langle K\rangle=K_1+K_2=0.60^{+0.02}_{-0.05}$ is in the allowed region.

IV. SUMMARY AND DISCUSSIONS

(1) We have made an estimate of the inelasticity distribution of hadron-Pb collisions, using 66 experimental events with energies $E\geqslant30$ TeV induced by cosmic ray hadrons. Based on the observed energy spectrum (with the exponent of -1.8 in integral form) and the obtained value of the inelasticity, these energies correspond to the $E_0>100$ TeV and $\langle E_0\rangle=2.3\times10^2$ TeV for the hadrons incident upon the chamber.

The average value of inelasticity is $\langle K\rangle=0.60^{+0.02}_{-0.05}$ and the distribution of the best fitting is

$$g(K)dK=[\alpha(1-K)^{m_1-1}+\beta K^{m_2-1}]dK,$$

with $m_1=0.5, m_2=1.125, \alpha=0.26, \beta=0.55$ (see Fig. 7). The method of estimation is independent of the absolute value of the shower energy.

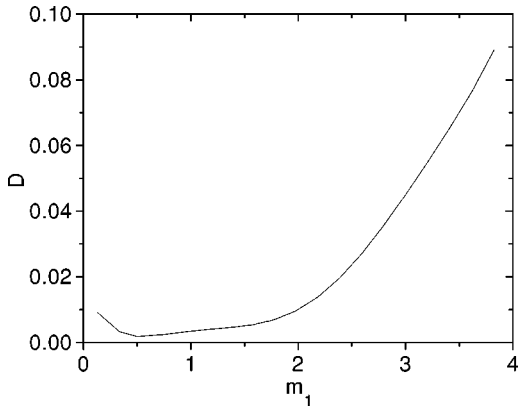

FIG. 6. Dispersion between the z distributions of the experiment and the calculation, for the various values of m_1 keeping $K_1=0.60$ and $K_2=0.0$ (consequently $\langle K\rangle=0.6$). The best fitting is attained at $m_1=0.5$.

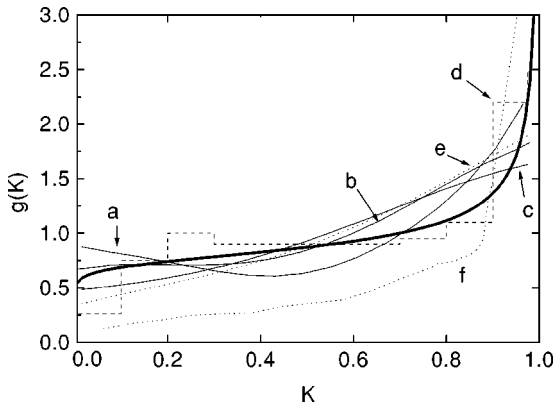

FIG. 7. Inelasticity distribution of the best fitting (the thick solid line), with $m_1=0.5, K_1=0.6, K_2=0.0$. The thin solid lines (*a, b, and c*) correspond to the cases of $m_1=1.0$, 1.5, and 2.0 (with $K_1=0.60$ and $K_2=0.0$), respectively. The chain line (*d*) corresponds to the case of $m_1=0.5$ with $K_1=0.55$ and $K_2=0.05$ (consequently $\langle K\rangle=0.6$). The dotted lines (*e* and *f*) are the calculations, based on the theoretical models by Hama and Paiva and by Tamada, respectively.

(2) The average value $\langle K\rangle=0.60^{+0.02}_{-0.05}$ of hadron-Pb collision at $E_0=2.3\times10^{14}$ eV is similar to the value 0.63 (at $\sqrt{s}=6.8\times10^2$ GeV) obtained by Hama and Paiva [24], but smaller than 0.82 (at $E_0=100$ TeV) estimated by Tamada [25]. The former calculation has been made on the basis of the interacting gluon model, and the latter on the basis of the geometrical model for hadron-nucleus interactions and the UA5 simulation code for particle production.

The average inelasticity $\langle K\rangle$ in *p*-Pb collisions at $E=100$ TeV is around 0.75 both in VENUS and QGSJET simulation codes [26]. Comparison of the *z* distribution with that made by VENUS and QGSJET codes tells that $\langle K\rangle$ is smaller in the experimental data than in simulations, and is consistent with the present one. Details of the analysis using VENUS and QGSJET codes will be described in succeeding papers.

(3) The distribution of the inelasticity is presented in Fig. 7. The inelasticity distributions for $m_1=0.5$ (the best fit), 1.0, 1.5, 2.0 in the case of $\langle K\rangle=0.6$ (with $K_1=0.6$ and $K_2=0$) have the value of *D* within allowed region ($D<0.01$), and they are similar to each other. The distribution obtained by Hama and Paiva is similar to these, too. The one from Ref. [25] is different reasonably, because of the difference of the average inelasticity.

There may be a peak at $K\sim0$ due to diffraction processes, which are not observable by the emulsion chamber experiment. Therefore the average inelasticity, estimated by the present data, is for non-single-diffractive events.

(4) In the present analysis the inelasticity is assumed to consist of two parts, i.e., $\langle K\rangle=K_1+K_2$. This corresponds to the experimental data of hadron-nucleus collisions which shows that the energy spectrum of produced particles is described by that of the *p*-*p* collision with an enhancement in the central region. Our analysis shows that $K_2<0.07$ belongs to the allowed region keeping $\langle K\rangle=0.60$. It follows that $K_1=0.53\sim0.6$, which is an approximate estimate of the inelasticity of hadron-nucleon collision for non-single-diffractive events.

The following comments are available for comparison of the above estimate with other data. (1) The value is slightly larger than the value of ~0.5 for non-single diffractive events, estimated by the UA5 group. (2) There has been a report that $dN/d\eta$, where η is pseudorapidity, is higher in the forward region than that of the UA5 data (16% excess at $\eta=4.1$) at $\sqrt{s}=630$ GeV for all inelastic events [27]. If $dN/d\eta$ of non-single-diffractive events increases accordingly, the average value of the inelasticity becomes $1.16\times0.5=0.58$. However it is shown that $dN/d\eta$ of the UA5 data is consistent in the forward region with that of the UA7 data and also with emulsion chamber data [14]. The present method of analysis made with better statistics of the experimental events will settle the issue.

(5) Discussions on experimental details. (a) The parameter *z* depends only on the relative values of energies. Hence it is free from absolute calibration of energy and consequently more reliable. (b) We do not always observe such a simple transition curve as illustrated in Fig. 2. That is, in some experimental events the transition curve has a complicated behavior, mainly due to the superposition of showers caused by their close shower starting points. In such cases a simple fitting of the calculated transition curves is not found to determine the shower energy. However, the value ΣE_i does not depend seriously on the way of fitting, because it is identical to the total track length of electrons in the shower. (c) A hadron-induced shower has a larger lateral spread than a γ-induced one, owing to the transverse momenta of the produced particles which initiate the shower. In the present analysis the primary energy of the interaction is 10^{14} eV. Let us take a γ-ray, emitted in the central region, which has $x=10^{-3}$ and $p_{T\gamma}=0.2$ GeV/*c*. After traversing $h=10$ cm of the chamber, it has a lateral spread of

$$r=\frac{p_{T\gamma}}{xE_0}h=2\times10^{-2}\ \text{(cm)}=200\ (\mu\text{m}).$$

Hence the γ rays, emitted in the central region, are situated outside the photometric slit and do not contribute to the shower darkness. This effect, however, is negligible, because the shower darkness is produced dominantly by the high energy γ rays. (d) In addition to *z* there are many other possible parameters which can be related to the inelasticity, such as $E_i/\Sigma E_i, E_i/E_j$, etc. The quantity $(\Sigma E_i)/E_{\text{fam}}$, where E_{fam} is the total energy of the family, also could be proposed. One can see, however, that *z* is the best among them, because the definition of it is clearer than others. (e) Most of cosmic ray hadrons, incident upon the chamber, are either nucleons or charged pions, whose abundance is approximately equal at the altitude of the Pamir station. In this sense the estimated distribution of inelasticity is averaged by the relative abundance of incident hadrons.

In pion collisions one should consider the charge exchange process of the incident pion (i.e., $\pi^{\pm}\rightarrow\pi^0$), which makes the inelasticity distribution of pion collisions different from that of nucleon collisions. However, the effect is not significant when the inelasticity is large similar to the value obtained in this analysis, because the energy left to the surviving pion is small. (f) Limited thickness of the chamber for

hadron detection is corrected by taking into account the finite chamber thickness t in calculation of the total radiated energy in the chamber. (See the Appendix.)

(6) We assume in the calculation that all the produced particles in hadron-Pb collisions are pions, and hence $c=1/3$. The value c does not affect the energy ratio z strongly, because both, the numerator and the denominator, contain the value almost in a proportional way. In other words, an excess of γ rays over charged pions and the contribution of kaons in the forward region will have a small effect on the present estimation of the inelasticity.

(7) To describe some of experimental events, in Ref. [28] the following assumptions are proposed. (a) The inelasticity of hadron-Pb collisions is considerably smaller (i.e., ~ 0.4) than that usually assumed in the geometrical approach of hadron-nucleus interactions (i.e., ~ 0.8) or (b) the event is produced by a bundle of collimated hadrons with multiplicity of ~ 10. From our present analysis the assumption (a) seems to be less probable. And the evaluation of the assumption (b) will be made elsewhere, because it is out of the scope of the present paper.

ACKNOWLEDGMENTS

The authors would like to thank Professor I.V. Rakobolskaya, Moscow State University group and the Pamir Collaboration for free use of data from the Pamir thick lead chambers. They also express their gratitude to Professor Y. Hama (Universidade de São Paulo), Professor T. Kodama (Universidade Federal Rio de Janeiro), and Professor G. Wilk (Soltan Institute of Nuclear Studies, Warsaw) for their valuable discussion and comments. One of the authors (V.K.) would like to thank Professor S. Hasegawa for his long term great support throughout the joint experimental work. We are grateful to FAPESP (Fundação de Amparo à Pesquisa do Estado de São Paulo) and FAPERJ (Fundação de Amparo à Pesquisa do Estado de Rio de Janeiro) for the financial support in part (Processos 1995/1192-0, 1995/9359-1,1995/9360-0, and 1998/E-26/150-529).

APPENDIX

A hadron of energy E_0, incident upon the chamber, causes a nuclear collision — multiple particle production — with Pb of the chamber. The surviving hadron and the produced hadrons collide again with Pb in the chamber at various depths in the chamber. These collisions initiate respectively cascade showers and those with the energy exceeding E_{th} are detected by the chamber. The observed energies of the showers are $E_1^{(\gamma)}$, $E_2^{(\gamma)}$, $E_3^{(\gamma)}$, ...

Let K be the inelasticity of the first interaction. Then we have

$E_1^{(\gamma)}=cKE_0$: the observed energy of the shower due to the first interaction, $(1-K)E_0$: the energy of the surviving hadron after the first interaction, $\varphi(x,\xi_1,\xi_2)dx$: the energies of the produced charged pions in the first interaction. (ξ_1 and ξ_2 are related to the inelasticity K.) The energy sum of all the observed showers is expressed as

$$\sum_1^n E_i^{(\gamma)}=E_1^{(\gamma)}+R(E_0,K) \quad \text{where} \quad R(E_0,K)=\sum_2^n E_i^{(\gamma)}.$$

The second term on the right-hand side $R(E_0,K)$ consists of the energies of the showers, except the first shower. These showers are produced by the collisions of the surviving hadron and the charged pions, all of which are produced in the first interaction with the inelasticity K.

We calculate $R(E_0,K)$ in an analytic way. The procedure is similar to the propagation of hadrons in the atmosphere [29], if one replaces the material of the air with the lead. That is, the surviving nucleon with the energy $(1-K)E_0$ causes collisions successively while traversing the chamber. Both the electromagnetic component (mainly via decays of π^0's) and the hadronic component are produced in their respective collisions. The electromagnetic component in respective collisions initiates cascade showers which are detected by the chamber. The hadronic component causes collisions again, but they are neglected in the calculation, because most of the secondaries have low energies compared with the detection threshold. The processes are the same for the charged pions, which are produced in the first interaction with the energy distribution $\varphi(x,\xi_1,\xi_2)dx$.

In the present section we describe the features of hadron-Pb collisions, present the number of nucleons and charged pions at the depth t in the chamber, and derive the formula for the energy sum of showers (except the first one), $R(E_0,K)$.

Features of hadron-Pb collisions. (1) Energy spectrum of the produced particles: The final state of nucleon-Pb collision of the inelasticity K consists of the surviving nucleon of energy $(1-K)E_0$ and charged pions with an energy spectrum $\varphi(x,\xi_1,\xi_2)dx$ of Eq. (1) in the text. The inelasticity distribution is expressed by Eqs. (2), (3), and (4). We assume that the energy spectrum of produced particles is the same in N(nucleon)-Pb as in π(pion)-Pb collisions. (2) Mean free path of the hadron-Pb collision. We assume that the mean free paths of N-Pb and π-Pb collisions are equal, because the size difference between the nucleon and pion has only a slight effect owing to the large size of Pb nucleus.

$$\lambda_N=\lambda_\pi\equiv\lambda=18.5 \ \text{(cm)}.$$

(3) The charge exchange of the incident pion into π^0. The charge exchange process in the case of pion incidence is important because there is a possibility that the surviving pion is a π^0, which results in a larger inelasticity. We assume that the charge exchange probability of the incident pion into π^0 is $b=1/3$.

Number of nucleons and charged pions in the chamber. When a single nucleon (or pion) of energy E_0 enters the chamber, a number of nucleons and charged pions are expected at depth t in the chamber through the nuclear collisions of the incident hadron. The expected number of nucleons $F_N(E,t)dE$ [or that of pions $F_\pi(E,t)dE$] with the energy E at the depth t in the chamber is given by the complex integrals of [29]

$$F_N(E,t)=\frac{1}{2\pi i}\int ds\left(\frac{E_0}{E}\right)^s\frac{1}{E}e^{\mu_N(s)\tau},$$

$$F_\pi(E,t)=\frac{1}{2\pi i}\int ds\left(\frac{E_0}{E}\right)^s\frac{1}{E}e^{\mu_\pi(s)\tau},$$

where $\tau=t/\lambda$. These are the solutions of the diffusion equation for the propagation of nucleons and charged pions in the chamber. In the above formulas

$$\mu_N(s)=1-\langle(1-K)^s\rangle \text{ and } \mu_\pi(s)=1-(1-b)\langle(1-K)^s\rangle$$

are the attenuation mean free paths of nucleons and pions, respectively. The brackets mean the average value, defined as

$$\langle(1-K)^s\rangle=\int_0^1(1-K)^s g(K)dK,$$

where $\langle x\rangle$ is the averaged value of the quantity x with respect to the distribution of the inelasticity $g(K)dK$.

Hence, in the case when the surviving nucleon has the energy $(1-K)E_0$ and the energies of the charged pions are distributed as $\varphi(x,\xi_1,\xi_2)dx$, the number of nucleons (pions) at the depth t in the chamber is given by

$$F_N(E,t)=\frac{1}{2\pi i}\int ds\left(\frac{(1-K)E_0}{E}\right)^s\frac{1}{E}e^{\mu_N(s)\tau},$$

$$F_\pi(E,t)=\frac{1}{2\pi i}\int ds\left(\frac{E_0}{E}\right)^s\frac{1}{E}\phi(s,\xi_1,\xi_2)e^{\mu_\pi(s)\tau},$$

where

$$\phi(s,\xi_1,\xi_2)=\int_0^1 x^s\varphi(x,\xi_1,\xi_2)dx.$$

Derivation of $R(E_0,K)$. The nucleons at a depth t cause nuclear collisions between t and $t+dt$. The number of collisions is given by

$$\frac{dt}{\lambda}F_N(E',t)dE'.$$

In these collisions the incident nucleons have energies E', and hence the showers, initiated by these collisions, have observed energies $cK'E'$, where the inelasticity K' is distributed as $g(K')dK'$. Consequently, the number of the showers with the energy E, which are produced at a depth t in the chamber is given by

$$dE\int_E^\infty\int_0^1\delta(E-cK'E')F_N(E',t)dE'\frac{dt}{\lambda}g(K')dK'.$$

The same consideration is applicable to the charged pions $F_\pi(E',t)dE'$. The difference between the nucleons and pions is that there exists a charge exchange (with the probability b) of the surviving particle for the pions. The shower energies are $cK'E'+(1-K')E'$ and $cK'E'$ for the cases with and without charge exchange, respectively.

Inclusion of the charge exchange process in the calculation is straightforward, and the number of the showers, which are produced at the depth t with the energy E by the collisions of nucleons and pions is given by

$$\begin{aligned}
&P_s(E,t)dEdt\\
&=dE\int_E^\infty\int_0^1\delta(E-cK'E')F_N(E',t)dE'\frac{dt}{\lambda}g(K')dK'\\
&\quad+dE\int_E^\infty\int_0^1[b\,\delta(E-[(1-K')+cK']E')\\
&\quad+(1-b)\,\delta(E-cK'E')]F_\pi(E',t)dE'\frac{dt}{\lambda}g(K')dK'\\
&=dEd\tau\int_0^1 g(K')dK'\left[\frac{1}{cK'}F_N\left(\frac{E}{cK'},t\right)\right.\\
&\quad+\frac{b}{(1-K')+cK'}F_\pi\left(\frac{E}{(1-K')+cK'},t\right)\\
&\quad\left.+\frac{1-b}{cK'}F_\pi\left(\frac{E}{cK'},t\right)\right]\\
&=dEd\tau\frac{1}{2\pi i}\int ds\left(\frac{E_0}{E}\right)^s\frac{1}{E}[(1-K)^s\langle(cK')^s\rangle\\
&\quad\times e^{\mu_N(s)\tau}\{b\langle[(1-K')+cK']^s\rangle\\
&\quad+(1-b)\langle(cK')^s\rangle\}\phi(s,\xi_1,\xi_2)e^{\mu_\pi(s)\tau}],
\end{aligned}$$

where $\langle x\rangle$ is the averaged value of the quantity x with respect to the distribution $g(K)dK$. One should be careful of the difference between K' and K through the derivation above. (K is the inelasticity of the first interaction and is not integrated here.)

The total observed energy of the showers except the first one, denoted as $R(E_0,K)$, is given by

$$\begin{aligned}
R(E_0,K)&=\int_0^t dt\int_{E_{th}}^\infty dE\,E\times P_s(E,t)\\
&=\frac{1}{2\pi i}\int\frac{ds}{s-1}\left(\frac{E_0}{E_{th}}\right)^s E_{th}\left[(1-K)^s\langle(cK')^s\rangle\right.\\
&\quad\times\frac{e^{\mu_N(s)\tau}-1}{\mu_N(s)}\{b\langle[(1-K')+cK']^s\rangle\\
&\quad\left.+(1-b)\langle(cK')^s\rangle\}\phi(s,\xi_1,\xi_2)\frac{e^{\mu_\pi(s)\tau}-1}{\mu_\pi(s)}\right].
\end{aligned}$$

Because $K=\xi_1+(1-\xi_1)\xi_2$, we can calculate $R(E_0,K)$ by assuming various types of distributions $f_1(\xi_1)d\xi_1$ and $f(\xi_2)d\xi_2$.

[1] For example, G.M. Frichter, T.K. Gaisser, and T. Stanev, Phys. Rev. D **56**, 3135 (1997).
[2] G.N. Fowler, R.M. Weiner, and G. Wilk, Phys. Rev. Lett. **55**, 173 (1985); G.N. Fowler, A. Vourdas, R.M. Weiner, and G. Wilk, Phys. Rev. D **35**, 870 (1987); G.N. Fowler, F.S. Navarra, M. Plümer, A. Voudras, R.M. Weiner, and G. Wilk, Phys. Rev. C **40**, 1219 (1989).
[3] Yu.M. Shabelski, R.M. Weiner, G. Wilk, and Z. Włodarczyk, J. Phys. G **18**, 1281 (1992); Z. Włodarczyk, *ibid.* **21**, 281 (1995).
[4] T.T. Chou and C.N. Yang, Phys. Rev. D **32**, 1692 (1985).
[5] T.K. Gaisser and T. Stanev, Phys. Lett. B **219**, 375 (1989).
[6] A.B. Kaĭdalov and K.A. Ter-Martirosyan, Proceedings of the 20th International Cosmic Ray Conference, 1987, Vol. 5, p. 139; Sov. J. Nucl. Phys. **40**, 135 (1984).
[7] R.A.M.S. Nazareth, T. Kodama, and D.A. Portes, Jr., Phys. Rev. D **46**, 2896 (1992).
[8] G. Schatz, T. Thouw, K. Werner, J. Oehlschläger, and K. Bekk, J. Phys. G **20**, 1267 (1994).
[9] T.K. Gaisser, R.J. Protheroe, K.E. Turver, and T.J.L. McComb, Rev. Mod. Phys. **50**, 859 (1978), and the references therein.
[10] L. van Hove and S. Pokorski, Nucl. Phys. **B86**, 243 (1975).
[11] M. Akashi *et al.*, Prog. Theor. Phys. Suppl. **32**, 1 (1964).
[12] R. Feynman, Phys. Rev. Lett. **23**, 1415 (1969).
[13] F.E. Taylor, D.C. Carey, J.R. Johnson, R. Kammerud, D.J. Ritchie, A. Roberts, J.R. Sauer, R. Schafer, D. Theriot, and J.K. Walker, Phys. Rev. D **14**, 1217 (1976).
[14] A. Ohsawa, Prog. Theor. Phys. **92**, 1005 (1994).
[15] N. Arata, Nucl. Phys. **B211**, 189 (1983).
[16] T. Tabuki, Prog. Theor. Phys. Suppl. **76**, 40 (1983).
[17] Chacaltaya Emulsion Chamber Collaboration, J.A. Chinellato *et al.*, Prog. Theor. Phys. Suppl. **76**, 1 (1983).
[18] UA5 Collaboration, G.L. Alner *et al.*, Phys. Rep. **5,6**, 247 (1987).
[19] J. Nishimura, *Handbuch der Physik* (Springer, Berlin, 1967), Vol. 46/2, p. 1.
[20] T. Arisawa, Y. Fujimoto, S. Hasegawa, K. Honda, H. Ito, V.V. Kopenkin, H. Semba, M. Tamada, K. Yokoi, G.F. Fedorova, I.P. Ivanenko, A.K. Managadze, I.A. Mikhailova, E.G. Popova, I.V. Rakobolskaya, T.M. Roganova, L.G. Sveshnikova, and O.P. Strogova, Nucl. Phys. **B424**, 241 (1994).
[21] Chacaltaya and Pamir Collaboration, L.T. Baradzei *et al.*, Nucl. Phys. B **B370**, 365 (1992).
[22] V. Kopenkin and Y. Fujimoto, Nuovo Cimento C **19**, 1017 (1996); M. Moriya, Master thesis, Waseda University, 1997.
[23] S.L.C. Barroso, Y. Fujimoto, V. Kopenkin, M. Moriya, C. Navia, A. Ohsawa, E.H. Shibuya, and M. Tamada, Nucl. Phys. B (Proc. Suppl.) **52B**, 201 (1997); Proceedings of the 25th International Cosmic Ray Conference, 1997, Vol. 6, p. 41.
[24] Y. Hama and S. Paiva, Phys. Rev. Lett. **78**, 3070 (1997).
[25] M. Tamada, J. Phys. G **21**, 1387 (1995).
[26] J. Knapp, D. Heck, and G. Schatz, report of Institut fur Kernphysik, Forschungszentrum Karlsruhe, Wissenchafteliche Berichte FZKA 5828, 1996.
[27] R. Harr, C. Liapis, P. Karchin, C. Biino, S. Erhan, W. Hofmann, P. Kreuzer, D. Lynn, M. Medinnis, S. Palestini, L. Pesando, M. Punturo, P. Schlein, B. Wilkens, and J. Zweizig, Phys. Lett. B **401**, 176 (1997).
[28] M. Tamada and V.V. Kopenkin, Nucl. Phys. **B494**, 3 (1997).
[29] A. Ohsawa, Prog. Theor. Phys. Suppl. **47**, 180 (1971); T.K. Gaisser, *Cosmic Rays and Particle Physics* (Cambridge University Press, Cambridge, England, 1990).